Biochemical Pharmacology 233 (2025) 116779

Contents lists available at ScienceDirect

Biochemical Pharmacology

journal homepage: www.elsevier.com/locate/biochempharm

The novel use of the CFTR corrector C17 in muscular dystrophy: pharmacological profile and *in vivo* efficacy

Alberto Benetollo [a], Sofia Parrasia [b], Martina Scano [a], Lucia Biasutto [c], Andrea Rossa [d], Leonardo Nogara [e], Bert Blaauw [a,e], Francesco Dalla Barba [a], Paola Caccin [a], Marcello Carotti [a], Alessandro Parolin [a], Eylem Emek Akyürek [f], Roberta Sacchetto [f], Dorianna Sandonà [a,*]

[a] *Department of Biomedical Sciences, University of Padova, 35131 Padova, Italy,*
[b] *Department of Biology, University of Padova, 35131 Padova, Italy*
[c] *Neuroscience Institute – Italian National Research Council (CNR), Padova, Italy*
[d] *Department of Chemical Sciences, University of Padova, Padova 35131, Italy*
[e] *Venetian Institute of Molecular Medicine, University of Padova, Padova 35129, Italy*
[f] *Department of Comparative Biomedicine and Food Science, University of Padova, Legnaro 35020, Italy*

ARTICLE INFO

Keywords:
Small molecules
α-Sarcoglycanopathy
Rare disease
Missense mutations
ADME
Mouse model

ABSTRACT

Sarcoglycanopathies are rare forms of severe muscular dystrophies currently without a therapy. Mutations in sarcoglycan (SG) genes cause the reduction or absence of the SG-complex, a tetramer located in the sarcolemma that plays a protective role during muscle contraction. Missense mutations in *SGCA*, which cause α-sarcoglycanopathy, otherwise known as LGMD2D/R3, lead to folding defective forms of α-SG that are discarded by the cell quality control. Recently, we demonstrated how a small molecule called C17, initially identified as a CFTR corrector, can be re-used to ameliorate the dystrophic phenotype of a mouse model of α-sarcoglycanopathy. Here, we have examined the pharmacological profile of C17 by performing ADME (absorption, distribution, metabolism, and elimination) studies. Our data show that C17 is well-distributed to relevant organs like heart and skeletal muscle, and likely metabolized in the small intestine into hydrophilic and hydrophobic derivatives. Elimination occurs through faeces (unmodified and modified C17) and urine (modified forms). Interestingly, we detected a quantifiable amount of C17 in treated muscles 48 h after an acute parenteral administration. This led to design a regimen of chronic treatment with a reduced dosing frequency. The result was the recovery of muscle strength, thanks to the rescue of the SG-complex, despite containing a mutated subunit, at the level of the sarcolemma. Thus, we can conclude that CFTR corrector C17 has a reasonable pharmacological profile and great potential to become a valuable therapeutic option for LGMD2D/R3 and other forms of muscular dystrophy caused by folding defective but potentially functional proteins.

1. Introduction

Sarcoglycanopathies are rare recessive forms of limb girdle muscular dystrophies (LGMD2C-F, also known as LGMDR3-6) still incurable [1]. Presently, the standard therapeutic intervention is just symptomatic, involving physiotherapy, nocturnal respiratory support, cardiologic

Abbreviations: ACN, acetonitrile; ADME, absorption, distribution, metabolism and excretion; ako, alpha-KO; ANOVA, analysis of variance; AUC, area under the curve; CFTR, cystic fibrosis transmembrane conductance regulator; CHCM, mean cellular haemoglobin concentration; CK, creatine kinase; CYP450s, cytochromes P450; DME, drug-metabolizing enzyme; DMSO, dimethyl sulfoxide; HCT, haematocrit test; HDW, haemoglobin distribution width; H&E, hematoxylin and eosin; HGB, haemoglobin; HM, human hepatic microsomes; HS9, human hepatic S9 fraction; i.m., intramuscular; i.p., intraperitoneal; KO, Knock-Out; LGMD, limb girdle muscular dystrophy; LGMD2D/R3, alpha-sarcoglycanopathy; MCH, mean corpuscular haemoglobin; MCHC, mean corpuscular haemoglobin concentration; MCV, mean corpuscular volume; MH+, mass to charge ratio of the protonated form; MM, murine hepatic microsomes; MPV, mean platelet volume; MS9, mouse hepatic S9 fraction; NADPH, β-nicotinamide-adenine dinucleotide phosphate; PAPS, adenosine 3'-phosphate 5'-phosphosulfate; PDW, platelet distribution width; PLT, platelet count; RBC, red blood cells; RDW, red cell distribution; SD, standard deviation; SEM, standard error of mean; SG, sarcoglycan; ST, sulfotransferase; TA, Tibialis Anterior; TFA, trifluoroacetic acid; UDPGA, uridine 5′-diphosphoglucuronic acid; UGT, uridine-glucuronosyltransferase; WBC, white blood cells; WT, wild type.

* Corresponding author.
E-mail address: dorianna.sandona@unipd.it (D. Sandonà).

https://doi.org/10.1016/j.bcp.2025.116779
Received 15 October 2024; Received in revised form 18 December 2024; Accepted 23 January 2025
Available online 24 January 2025

surveillance/treatment and surgery (if necessary to resolve tendons retraction), in combination with corticosteroids administration [2,3]. Sarcoglycanopathies are progressive diseases, with the involvement of the proximal limb girdle musculature. The onset may range from childhood to early adulthood, but in the majority of cases, it occurs in the first decade of life [3,4]. Sarcoglycanopathies are caused by mutations in the sarcoglycan (SG) coding genes (*SGCA*, *SGCB*, *SGCG*, and *SGCD*). Large gene deletions, null and out of frame mutations are reported for all genes, even though the most frequently reported genetic defects are the missense mutations [5]. In this case the result is a folding defective SG that is recognized by the cell's quality control (QC) system and degraded through the endoplasmic reticulum associated degradation (ERAD) pathway [6]. The outcome is a strong reduction of the mutated subunit as well as of the wild type partners at the sarcolemma [7–10]. As part of the search for new therapeutic approaches for sarcoglycanopathies and considering the similar pathogenetic mechanism, we thought about the re-use of cystic fibrosis transmembrane conductance regulator (CFTR) correctors, small molecules able to recover folding and trafficking defective CFTR mutants [11]. This pharmacological approach for the treatment of LGMD2D/R3 seems very promising, as the successful recovery of α-SG missense mutants has been demonstrated both in cellular models, and in primary myogenic cells from a subject carrying the L31P/V247M mutations on the SGCA protein [12,13]. The use of these molecules evidenced that most of the missense mutants can be rescued at the plasma membrane, where they are functional. Indeed, LGMD2D/R3 myotubes treated with the corrector C17 are protected from the leakage of the cytosolic protein creatine kinase (CK) when subjected to stressful conditions [12]. Interestingly, among the different CFTR correctors tested, corrector C17 (Fig. 1), a bithiazole derivative, was identified as the most promising in sarcoglycanopathy, since it has broad activity on different SG mutants and primarily, because it is effective in ameliorating the myopathic features of a LGMD2D/R3 murine model after a chronic treatment of five weeks [14]. Notably, the muscle strength of these mice was significantly improved, highlighting the great potential as a drug candidate for sarcoglycanopathies [14]. The purpose of this work is the in-depth investigation of the pharmacological properties of corrector C17 as, to the best of our knowledge, no such data are available in the literature. To this intent, we performed *in silico* metabolite prediction [15,16], *in vitro* biotransformation assays to verify metabolite(s) generation [17] and *in vivo* pharmacokinetics experiments. Thus, the bithiazole compound has been characterized in all four phases involved in ADME (absorption, distribution, metabolism, elimination) studies by exploiting the intraperitoneal (i.p.) administration in mice [18]. Data from ADME studies allowed us to design a novel protocol of treatment to evaluate C17 efficacy. Haematological, biochemical and functional parameters have been assessed after the chronic treatment.

2. Materials and methods

2.1. Chemicals and reagents

CFTR corrector C17 was purchased from Exclusive Chemistry (Kiryat Motzkin, Israel), Kolliphor-EL, DMSO, phosphate buffered saline 10X pH 7.4 (PBS), HEPES, $MgCl_2$, PMSF and EDTA were from Sigma-Aldrich (St. Louis, MO, USA), Alamethicin from Life Technologies (Monza, Italy). Pooled human liver microsomes, mixed gender (098H0620) and pooled human liver S9 fraction, mixed gender (098H0620.S9) were from Tebubio (Magenta, Italy). The cofactors UDPGA (Uridine 5′-diphosphoglucuronic acid trisodium salt; U-6751), NADPH (β-nicotinamide-adenine dinucleotide phosphate, tetrasodium salt), and PAPS (adenosine 3'-phosphate 5'-phosphosulfate, tetralithium salt) were purchased from Merck (Milan, Italy). Resveratrol was from Sigma-Aldrich (St. Louis, MO, USA). HPLC-grade acetonitrile (ACN) and trifluoroacetic acid (TFA) were obtained from Carlo Erba (Milan, Italy) and used without further purification. The SMonovette® K3 EDTA tubes for blood collectionwere from Sarstedt (Numbrecht, Germany).

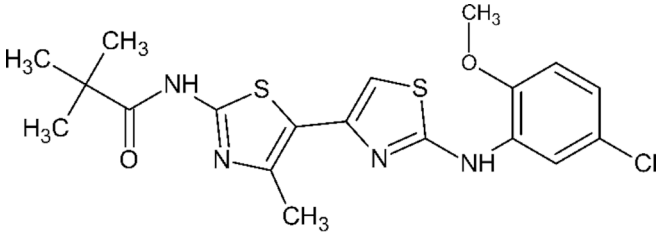

Fig. 1. Chemical structure of C17.

2.2. In silico metabolism prediction analysis: Biotransformer 3.0

For initial metabolism simulation, the online Biotransformer 3.0 tool was used [15,16]. The software was operated in CYP450 (or Phase I), Phase II and Human Gut mode, and two consecutive reaction steps were performed. SMILES was used as input format.

2.3. Chemical structures of CFTR corrector C17 and its predicted metabolites

All chemical formula present in the article were generated by using the software ACD/ChemSketch developed by the Advanced Chemistry Development, Inc. (ACD/Labs) [38]. Furthermore, after the *in silico* metabolism prediction analysis, the software ACD/ChemSketch was exploited also to calculate the mass to charge ratio of the protonated form ($[M + H]^+$), henceforth MH^+, of the predicted metabolites. These molecules were merged with the C17-derived compounds identified in urine, faeces and small intestine content of mice treated with C17, thus allowing to define which species were actually formed *in vivo*.

2.4. In vivo experiments

All procedures were performed in accordance with the European guidelines and regulations for the human care and use of experimental animals, and conducted with the supervision of the Central Veterinary Service of the University of Padova, in compliance with Italian Law DL 26/2014, embodying UE Directive 2010/63/EU. The protocol has been authorized by the Public Veterinary Health Department of the Italian Ministry of Health (Authorization n°24/2020-PR, 10/01/2020). C57BL/6 and *sgca*-null mice were used for testing the blood stability, biotransformation, biodistribution, and elimination, and for the chronic treatment with C17. Animals provided with water and food *ad libitum*, were housed in a thermally controlled room at 20-24 °C with a light/dark cycle of 12 h. Both male and female mice, chosen randomly, were used for this study. The murine model of alpha-sarcoglycanopathy used in the chronic treatment was generated by intramuscularly injecting the viral vector (AAV1) that carries the human R98H-α-SG cDNA sequence into the hind limbs of *sgca*-null mice aged 24 to 48 h, as described in [14]. For chronic treatments, 7 weeks-old mice with humanized hind limbs were injected intraperitoneally (i.p.) for 5 weeks every 48 h with either 25 mg/kg of C17 in formulation with 5 % DMSO, 5 % Kolliphor-EL in physiological solution or the vehicle formulation.

2.5. HPLC-UV (Ultraviolet) analysis

Quantitative analyses of solutions resulting from the work-up of tissue or blood samples were carried out by HPLC/UV (1290 Infinity LC System, Agilent Technologies, Milan, Italy) exploiting a reversed-phase column (Zorbax RRHT Extend C18, 1.8 μm, 50 x 3.0 mm, Agilent Technologies) and a UV diode array detector (190–500 nm), at a flow rate of 0.6 mL/min. Solvents A and B were water + 0.1 % TFA and ACN, respectively. The gradient for B was as follows: 10 % for 1 min, then

from 10 to 100 % in 7.0 min, 100 % for 0.5 min, then from 100 % to 10 % in 1.5 min. The injection volume was 5 μL. The eluate was preferentially monitored at 312 nm (corresponding to an absorbance maximum of C17 compound). The temperature of the column was kept at 25° C.

2.6. C17 extraction procedure from tissues and plasma and recovery yields

Liver, kidneys, spleen, heart, lungs, skeletal muscle and brain obtained from mice were weighed and about 100 mg of tissues were homogenized with PBS pH 7.4 (1 vol) with a pellet pestle (Pellet pestles Cordless motor, Sigma-Aldrich). After vortexing, 2.5 vol of acetone were added and the sample was sonicated for 2 min. Subsequently, 2.5 vol of acetonitrile containing 0.1 % TFA were added and the sample was sonicated for 5 min. The sample was then centrifuged at 12,000×*g* for 7 min at 4° C, the supernatant was collected, and analyzed via HPLC-UV.

Preliminary experiments were performed adding a pre-established amount of C17 into tissue homogenates or blood (100 μL) from untreated mice, and evaluating the recovery yields of C17 from tissues and plasma using the extraction procedure described above. The concentration of the analyte in the sample was calculated from the calibration curve (Peak area (312 nm), 6.33 × Concentration (μM)).

The volume of the sample analyzed was carefully measured to calculate the amount of analyte: μmol, concentration (μM) × Volume (L).

The recovery yields were calculated as follows: (total μmol quantified via HPLC/μmol spiked) × 100.

The recovery yields for liver, kidney, spleen, heart, lung, skeletal muscle, brain and blood were 87.1 ± 2.0 %, 75.3 ± 0.6 %, 88.1 ± 3.9 %, 85.0 ± 4.6 %, 78.1 ± 2.9 %, 76.8 ± 3.8 %, 85.8 ± % 6.2, and 91.7 ± 4.4 %, respectively.

2.7. Blood stability

C57BL/6J mice were anaesthetized and blood was withdrawn from the jugular vein into S-Monovette® K3 EDTA, 1.2 ml (Sarstedt). Blood samples (1 mL) were spiked with compound (25 μM; dilution from a 25 mM stock solution in DMSO) and incubated at 37° C for 4 h under agitation (370 rpm) in a ThermoShaker. 100 μl aliquots were taken after 0, 0.5, 2, and 4 h, treated as described above and analyzed by HPLC-UV.

2.8. Tissue distribution studies

C17 was administered as a single intraperitoneal dose (25 mg/kg body weight, dissolved in saline solution with 5 % DMSO and 5 % Kolliphor EL) to C57BL/6J mice. At different time points after compound administration (0.25, 2, 6, 24, and 48 h), animals were anesthetized and sacrificed (n, 3 for each time point). Blood was collected in heparinized tubes, kept in ice and treated as described above within 10 min from sampling. Liver, kidneys, spleen, heart, lungs, skeletal muscle and brain were removed, weighed, and immediately frozen in liquid nitrogen; extraction and analyses were then performed as described above. The area under the curve (AUC) values were calculated using the trapezoidal rule.

2.9. Hepatic microsomes and S9 fraction isolation from mouse liver

An appropriate number of livers were harvested from *sgca*-null mice and immediately frozen in liquid nitrogen. The organs were stored at −80 °C until further processing. The livers were homogenized initially in the homogenization buffer (sucrose 0.250 M, HEPES 50 mM, KCl 25 mM, MgCl 5 mM, EDTA 0.1 mM, pH 7.4) in the presence of serine protease inhibitor PMSF 0.1 M in EtOH (250 μM) by using the Ultra Turrax T25 at 20,500 rpm for 4 times for 30 s at 4 °C. S9 fraction was obtained by centrifugation of the homogenate at 800×*g* for 10 min at 4 °C, then supernatant was centrifuged at 12,000×*g* for 15 min at 4 °C. The supernatant corresponding to S9 fraction was decanted and protein concentration was determined through the Pierce BCA assay (ThermoFisher). To obtain microsomes, homogenates were centrifuged at 700×*g* for 10 min at 4 °C and then 10,000×*g* for 10 min at 4 °C. The pellet was discarded, and the supernatant was then centrifuged at 15,000×*g* for 20 min at 4 °C. The pellet was discarded again, and homogenates were re-centrifuged at 105,000×*g* for 1 h at 4 °C with ultracentrifuge (Optima max-XP, Beckman Coulter, Brea, California, United States). Following this high-speed step, the supernatant was discarded, and the pellet was resuspended in the homogenization buffer and centrifuged again at 105,000×*g* for 1 h at 4 °C. The supernatant was again discarded and the remaining pellet, corresponding to the microsomal fraction, was resuspended in the homogenization buffer. The Pierce BCA assay was performed to determine microsome-protein concentration. Microsomes and S9 fractions were stored at −80 °C until use.

2.10. In vitro biotransformation studies

Incubations for *in vitro* biotransformation studies were conducted in a reaction mixture containing: 5 μM (final concentration) C17 compound and 0.5 mg/ml microsomes (human/mouse) or 2.5 mg/ml S9 fraction (human/mouse) in reaction buffer (0.1 M potassium phosphate buffer, KPB solution (pH 7.4), $MgCl_2$ 5 mM, EDTA 1 mM) maintained at 37 °C in a ThermoShaker. Resveratrol was used as a positive control. Cofactors, NADPH (1 mM), UDPGA (2 mM), and PAPS (0.5 mM), were added individually or as a cocktail mixture. Before starting incubations, microsomes or S9 fractions were incubated for 30 min with alamethicin (final concentration, 50 μg/mL) to activate uridine-glucuronosyltransferases (UGTs). After 5 min of incubation at 37 °C, cofactor(s) were added to the reaction mixture containing the compound. The total DMSO concentration in the reaction solution was 1 % (v/v). Aliquots (100 μl) from the reaction mixtures were sampled at 0 and 60 min, and ice-cold acetonitrile + 0.1 % TFA (1 vol) was added to quench the reaction. After vortexing, samples were sonicated for 2 min and then centrifuged at 12,000×*g* at 4 °C for 7 min, and the supernatant was analyzed by HPLC/UV. For the human *in vitro* biotransformation studies, pooled human liver microsomes and human liver S9 fractions were used.

2.11. Urine, faeces and gut content collection

C17 (25 mg/kg) or vehicle were intraperitoneally administered to C57BL/6J mice and urine and faeces were collected by exploiting the spot sample collection method after 18 h and 24 h, respectively [19]. The gut content was collected 24 h post injection by performing a midline incision to access the gut, and then the whole small intestine (duodenum, jejunum, ileum) tract was removed. Biological samples were weighted, homogenized with PBS pH 7.4 (1 vol for urine, 2 vol for faeces), and processed as previously described. Then, the supernatant was collected and analyzed via HPLC-UV and eventually HPLC-UV/Electrospray Ionization–Mass Spectrometry (ESI-MS).

2.12. HPLC-UV/electrospray ionization–mass spectrometry (ESI-MS)

Identification of C17 metabolites in faecal and urine extracts was carried out with an 1100 Series Agilent Technologies system. HPLC-UV/ESI-MS analysis of selected biological sample extracts was carried out using a reversed-phase HPLC column (Kinetex C18, 5 m, 150 4.6 mm, 100 Å, Phenomenex) and a flow rate of 1.0 mL/min. Solvents A and B were water + 0.1 % formic acid and ACN + 0.1 % formic acid, respectively. The gradient for B was as follows: 3 min at 10 %, from 10 % to 100 % in 27 min, then 100 % for 2 min. The eluate was monitored at 312 nm. Alternatively, a linear gradient from 10 % to 100 % B in 20 min was used. MS analysis was performed with an ESI source operating in full-scan positive ion mode, applying the following ESI parameters: nebulizer pressure 50 psi, dry gas flow 8 L/min, dry gas temperature 350 °C.

2.13. Muscle physiology

For *in vivo* force measurement procedure, the animal was anesthetized with an intraperitoneal injection of ketamine 100 mg/kg xylazine 10 mg/kg and, a few minutes later, an intramuscular injection of tramadol 5–10 mg/kg was performed as a pain relief treatment. A small incision was made on the side of the knee to the direction of the hip, exposing the common peroneal nerve. A teflon-coated seven-stranded steel wire (AS 632; Cooner Wire Company, Chatsworth, CA, USA) was sutured with 5–0 silk thread at each side of the common peroneal nerve. Upon electrical stimulation, torque production of the TA muscle is measured using a lever system (Model 305B; Aurora Scientific, Aurora, ON, Canada). The electrical stimulation has been performed on a S88 stimulator (Grass Instrument, Warwick, RI, USA) using the following protocol: train duration 200 ms, pulse width 500 μs, 1–2 V and stepwise increase frequencies from a single pulse to 20, 40, 55, 75, 100 and 150 Hz; each train is performed every 30 s to avoid effects due to fatigue. TA muscles from C57BL/6 and *sgca*-null mice of similar age and weight were used as positive and negative control, respectively. After force measurements, mice were sacrificed by cervical dislocation, blood was drawn from the orbital sinus for biochemical and haematological analyses and muscles were dissected, weighed and frozen in isopentane precooled in liquid nitrogen for further analyses.

2.14. Immunofluorescence (IF) analyses

Immunofluorescent staining of α-SG and δ-SG was carried out to assess the cytolocalization of the proteins. From frozen muscle explants, transverse cross sections (10-μm thick) were cut in a cryostat microtome (Leica CM1850) set at − 24 ± 1°C. Muscle cryo-sections were washed and blocked with 10 % goat serum in 0.5 % bovine serum albumin (BSA) in PBS for 1 h at room temperature. Muscle sections were incubated overnight at 4 °C with the primary antibodies (all raised in rabbit) specific for α- and δ-SG diluted 1:2000 and 1:500 in 0.5 % BSA, respectively. Protein signals were revealed with an anti-rabbit Alexa-Fluor-488 (Invitrogen, Carlsbad, CA, USA) diluted 1:500 in 0.5 % BSA in PBS incubated for 2 h at room temperature. Nuclei were counterstained with DAPI (Abcam, Cambridge, UK). The Leica DMR fluorescence microscope equipped with a digital camera was used to examine muscle sections.

2.15. Antibodies

Rabbit monoclonal anti-α-SG (AB189254) was from Abcam (Cambridge, UK); rabbit polyclonal antibody specific for δ-SG was produced and characterized as previously described [10]. Fluorescent antibodies were Alexa Fluor 488-conjugated goat anti-rabbit IgG (Invitrogen, Carlsbad, CA, USA).

2.16. Haematological analysis

These analyses consisting of the complete red blood cells (RBC), white blood cells (WBC) and platelets count, kidney function evaluation (creatinine/UREA measurement), and muscle damage determination (creatine kinase, CPK, measurement) were performed at the Istituto Zooprofilattico Sperimentale delle Venezie (Legnaro, Padova, Italy).

2.17. Histological analysis of hearts

Hearts were fixed in buffered neutral paraformaldehyde at 4 °C, washed in phosphate-buffered saline and dehydrated through a graded series of ethanol. Samples embedded in paraffin were cut at 5 μm and stained with hematoxylin and eosin (H&E). Sections were clarified and mounted in Eukitt balsam (ORSA-tek, Germany) for microscopic examination. The images were acquired by the automated slide scanner (Axioscan 7, Zeiss, Germany) and analyzed with Zeiss ZEN Microscopy Software (Zeiss, Germany). Heart analyses were carried out by measurement of the apicobasal length of the heart (AB) and the maximal heart width perpendicular to AB.

2.18. Statistical analysis

Data were expressed as means ± SD. For *in vivo* functional experiments, data were expressed as means ± SEM. Statistical differences among groups were determined by one-way ANOVA test, followed by Tukey's multiple comparisons test. When only two groups were considered, statistical analysis was performed by the unpaired two-tailed Student's *t*-test. A level of confidence of $P < 0.05$ was used for statistical significance.

3. Results

3.1. Blood stability

A drug molecule exerts the pharmacological effect over a satisfactory time period if it is sufficiently stable. Thus, blood stability is a key parameter to be investigated [20]. The C17 corrector (25 μM) was incubated for 4 h in blood maintained at 37 °C, the physiological temperature, and at different time points (0, 0.5, 2, and 4 h) aliquots of blood were collected and analyzed by HPLC/UV. After an initial reduction of about 15 % during the first 30 min, in the following 3.5 h of incubation C17 remained stable, with the detected amount of C17 being ~80–85 % compared to the amount initially detected at time 0 (Fig. 2). This behavior suggests that C17 is stable in the blood, notwithstanding the first drop, which may be due to interaction/absorption with the surface of the sample tube. Furthermore, the HPLC/UV analysis at different wavelengths (216, 250, 286, 312, 350, and 400 nm) did not reveal the formation of any new peaks corresponding to possible C17-derived metabolites.

3.2. Tissue distribution and blood steady-state level of C17

The concentration–time kinetic relationship in mice was determined after a single administration of C17 through the intraperitoneal route. Mice were sacrificed after 0.25, 2, 6, 24 and 48 h, and blood, organs and tissues were collected and analyzed. The quantification of the analyte

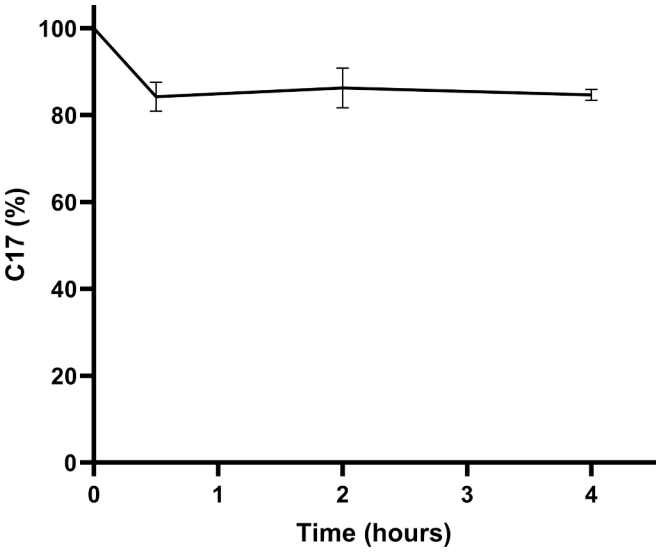

Fig. 2. Blood stability of CFTR corrector C17. In the graph is reported the percentage of remaining C17 at different time points (0, 0.5, 2, and 4 h), in comparison to the initial amount detected at time 0. The graph reports the mean value ± S.D. of 3 independent experiments each one done in triplicate.

C17, and/or its metabolites, was done considering the recovery yield from each tissue/organ analyzed (see Material and Methods). Fig. 3A shows the concentration of C17 in plasma and tissues as a function of time, while the graphs of Fig. 3B report the calculated areas under the curve at each time point, and the Research data report the C_{max} and t_{max} for the investigated analyte (n, 3 or 4 for each time point). We can speculate that C17 reaches firstly the most vascularized organs, such as the liver, kidney, and spleen, and then the analyte is redistributed to the whole body through blood circulation. Indeed, in the plasma, the maximum level of C17 (C_{max}) is reached 2 h post-injection. With the same kinetic observed in the blood, C17 reached the C_{max} after 2 h in skeletal muscle, heart, and brain, where it remained stable up to 6 h post-administration. Thus, the intraperitoneal injection of C17 resulted in a rapid distribution phase, followed by a prolonged elimination phase, with only traces of the compound present in plasma, brain, liver, lung, kidney and spleen 48 h post-injection. Of note, in skeletal muscle and heart, the target tissues for the treatment of sarcoglycanopathy, a residual amount (6.5 % of the C_{max}) of C17 was still present after 48 h. C17 derivatives were not detected in the analyzed tissues. The compound C17 is a very hydrophobic molecule, therefore its presence in plasma still at 48 h post-injection could be due to its binding to plasma proteins, as demonstrated for other CFTR correctors (Ivacaftor and Lumacaftor) [21], a feature that might significantly prolong the half-life of the compound.

The steady state of C17 concentration in plasma was determined by performing subsequent (daily) intraperitoneal injections in mice with the dosage of 25 mg/kg. The canonical plateau in terms of moles x plasma volume, which for the C17 corrector was ~ 2.0–2.2 nmol/mL, was reached after 3–5 days of daily injection (Fig. 3C).

3.3. *In silico metabolism studies*

To the best of our knowledge, the metabolism of C17 has never been studied, therefore as first step aiming at investigating its biotransformation, and (consequently) elimination mechanisms, an *in-silico* analysis was performed by using the tool Biotransformer 3.0, a freely available web server that combines machine learning approaches with a rule-based system to predict small-molecule metabolism. The server was run by selecting different metabolic transformations, as indicated in Fig. 4, in order to have the highest number of possible modifications to which the input molecule can undergo. We submitted the molecular structure of C17 as input and the server output was a list of the predicted metabolites along with the reaction equation(s), the reaction types and the enzymes that are predicted to be responsible for those reactions [16]. Predicted metabolites are reported in Research data.

3.4. *In vitro biotransformation studies*

The investigation of *in vitro* C17 metabolism was carried out by using both human and murine hepatic microsomes (HM and MM) and human and murine hepatic S9 fractions (HS9 and MS9). Hepatic fractions were activated by NAPDH, UDPGA, and PAPS as cofactors for CYP450s (cytochromes P450), UGTs (uridine-glucuronosyltransferases) and STs (sulfotransferases), respectively. Hepatic fractions were incubated for 60 min with the analyte and the cofactor(s) to ensure drug-metabolizing enzymes (DMEs) activation. Aliquots of the mixture collected after 0 and 60 min from the activation of DMEs were subsequently analyzed at the HPLC/UV. The analysis revealed that C17 is not metabolized in all the experimental conditions (Fig. 5A and B) either by activating just one family of enzymes or all three families of DMEs at the same time. In fact, no other HPLC/UV peaks other than C17 were identified in the chromatogram, and the amount of C17 remained unchanged during the entire experiment. Results for positive and negative controls are reported on Research data. These results showed that C17 is not metabolized *in vitro* by activated-DMEs of different human and mouse hepatic fractions, suggesting the compound could be eliminated as unmodified or after modification performed in an organ, different from liver, involved in the xenobiotic metabolism.

3.5. *Elimination studies*

3.5.1. *Determination of metabolites in urine*

Urine samples were collected from mice upon a single parenteral C17 administration using the spot-sample collection method [19]. Samples were first analyzed by HPLC/UV (Fig. 6A), followed by metabolite identification through mass spectrometry analysis (Fig. 6B-C). Two metabolites were detected in urine collected 18 h after C17 administration. The first metabolite ($MH^+ = 629.1$) could be the product of a two-step reaction: an O-dealkylation (M1) followed by an aromatic OH-glucuronidation (Fig. 6B). The second metabolite ($MH^+ = 599.1$) (Fig. 6C) could have originated from different metabolic reactions as indicated in Fig. 6D. These metabolites are glucuronides, and they present a higher level of hydrophilicity than the parental compound, in accordance with urinary elimination. In tissues analyzed during distribution studies, the metabolites were not detected, suggesting that these C17 derivatives might be generated in compartment(s) different from the liver, kidney or lung, the organs normally involved in drug biotransformation. On the other hand, it is known that xenobiotic metabolism can occur also in other tissues/organs like the intestine [22]. Thus, we suppose these metabolites were generated in the intestine, their re-absorption occurred at the level of the small intestine in which the re-absorption of water and hydrophilic molecules takes place, and were eventually eliminated through the urine.

3.5.2. *Determination of metabolites in faeces.*

Faeces of mice that underwent intraperitoneal administration with C17 were collected through the spot-sample method. Samples were analyzed by HPLC/UV followed by the ESI-MS analysis. In faeces collected 24 h after administration of C17, we identified two metabolites indicated as peaks 3 and 4 on the UV chromatogram of Fig. 7A, with MH^+ of 453.1 and 423.1, respectively (Fig. 7B-C). These two faecal metabolites were predicted *in silico*. The metabolite 3 ($MH^+ = 453.1$) (Fig. 7B) may result from the hydroxylation (6 *in silico* predicted metabolites) or the epoxidation (just 1 *in silico* predicted metabolite) reaction. The metabolite 4 ($MH^+ = 423.1$) (Fig. 7C) could have been generated by a reaction of O-dealkylation (M1). The metabolic pathways for these compounds are indicated in Fig. 7E. The precursor compound (C17) was detected as unmodified (peak C17 in the UV chromatogram, Fig. 7D), as we expected due to its hydrophobic properties.

3.5.3. *Determination of metabolites of the small intestine content*

To better understand the metabolic fate of our compound, we analyzed the small intestine content of mice treated with C17 after 24 h from intraperitoneal injection. The collected biological sample corresponding to the content of duodenum, jejunum, and ileum, contains a certain amount of water, and consequently also hydrophilic molecules that are typically reabsorbed at the level of the colon, thanks to its dehydrating activity [23]. The HPLC/UV analysis followed by ESI-MS (reported in Fig. 8A) revealed the presence of the unmodified compound C17 and the metabolites previously identified in urine and faeces (the comparison of the HPLC-UV chromatograms from small intestine content, urine and faeces is reported in Fig. 8B). In Fig. 8A, the extracted ion chromatogram of each detected compound is reported with the specific MH^+. Interestingly, we identified more than one metabolite with $MH^+ = 629.1$ (indicated as 1.1 and 1.2 in Fig. 8B) and $MH^+ = 453.1$ (indicated as 3.1 and 3.2 in Fig. 8B) suggesting that the glucuronidation and the hydroxylation (or epoxidation) may occur at different functional groups. The additional two metabolites correspond to the glucuronide ($MH^+ = 599.1$) and the O-dealkylated C17 ($MH^+ = 423.1$). No other metabolites were identified.

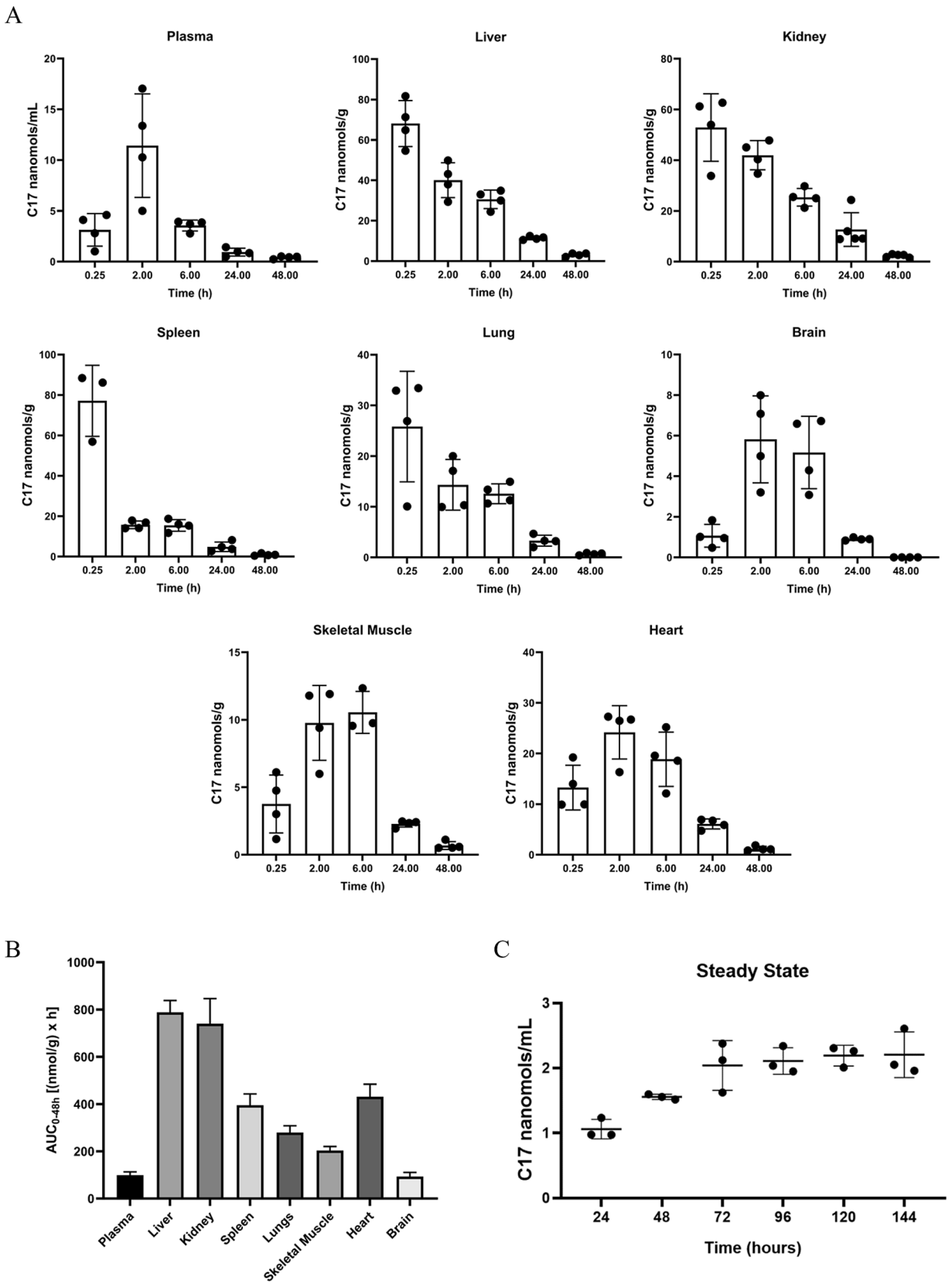

Fig. 3. Biodistribution studies and steady state concentration of CFTR corrector C17. (A) Concentration versus time profiles of C17 in plasma and tissues. After a single intraperitoneal injection of C17 (25 mg/Kg), mice were sacrificed at different time points (0.25, 2, 6, 24, and 48 h). Reported data are mean values ± S.D. (n = 3 or 4). (B) AUC values are plotted for plasma and various tissues/organs. Data are expressed as mean values ± S.D. (C) Steady state study: plasma concentration (nanomoles per milliliter) vs. time curve of C17 following repeated i.p. injection (25 mg/kg) in mice. Mice were injected daily with the same C17 dosage and sacrificed at different time points (24, 48, 72, 96, 120, 144 h).

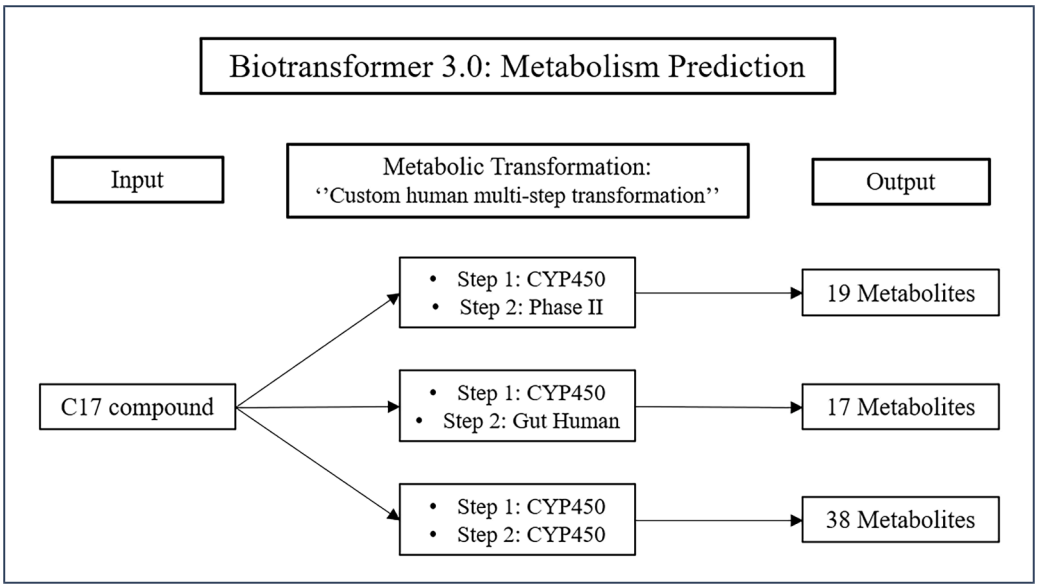

Fig. 4. C17 metabolism prediction with Biotransformer 3.0.. Schematic workflow of the settings to study the biotransformation of C17 compound by means of the Biotransformer 3.0 metabolism prediction tool.

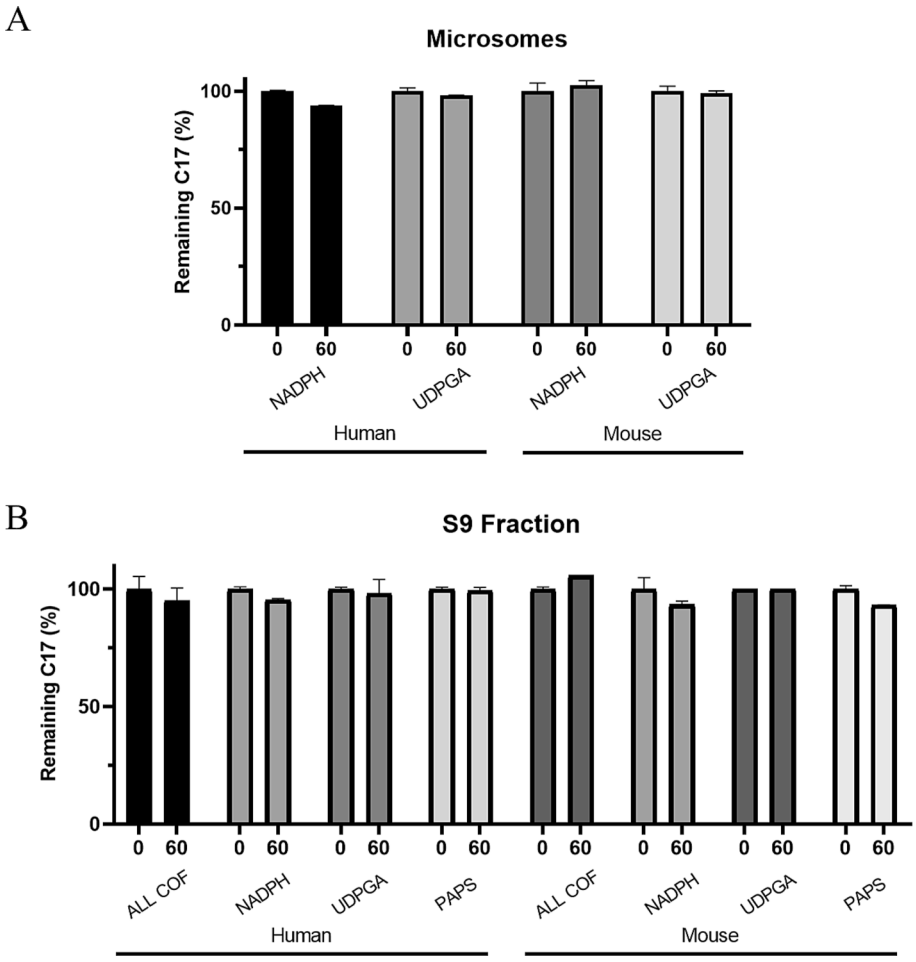

Fig. 5. *In vitro* metabolism investigation of C17 in human and mouse microsomes (A), and human and mouse S9 fraction (B). C17 (5 μM) was incubated with microsomes (0.5 mg/mL) or S9 fraction (2.5 mg/mL) for 60 min at 37 °C. Cofactors (NAPDH 1 mM, UDPGA 2 mM, and PAPS 0.1 mM) were added individually or as a cocktail (ALL COF, as indicated only for S9 fractions). Data are expressed as the percentage of C17 in comparison to the initial amount at time 0. The graph reports the mean value ± S.D. of 2 independent experiments each one done in duplicate.

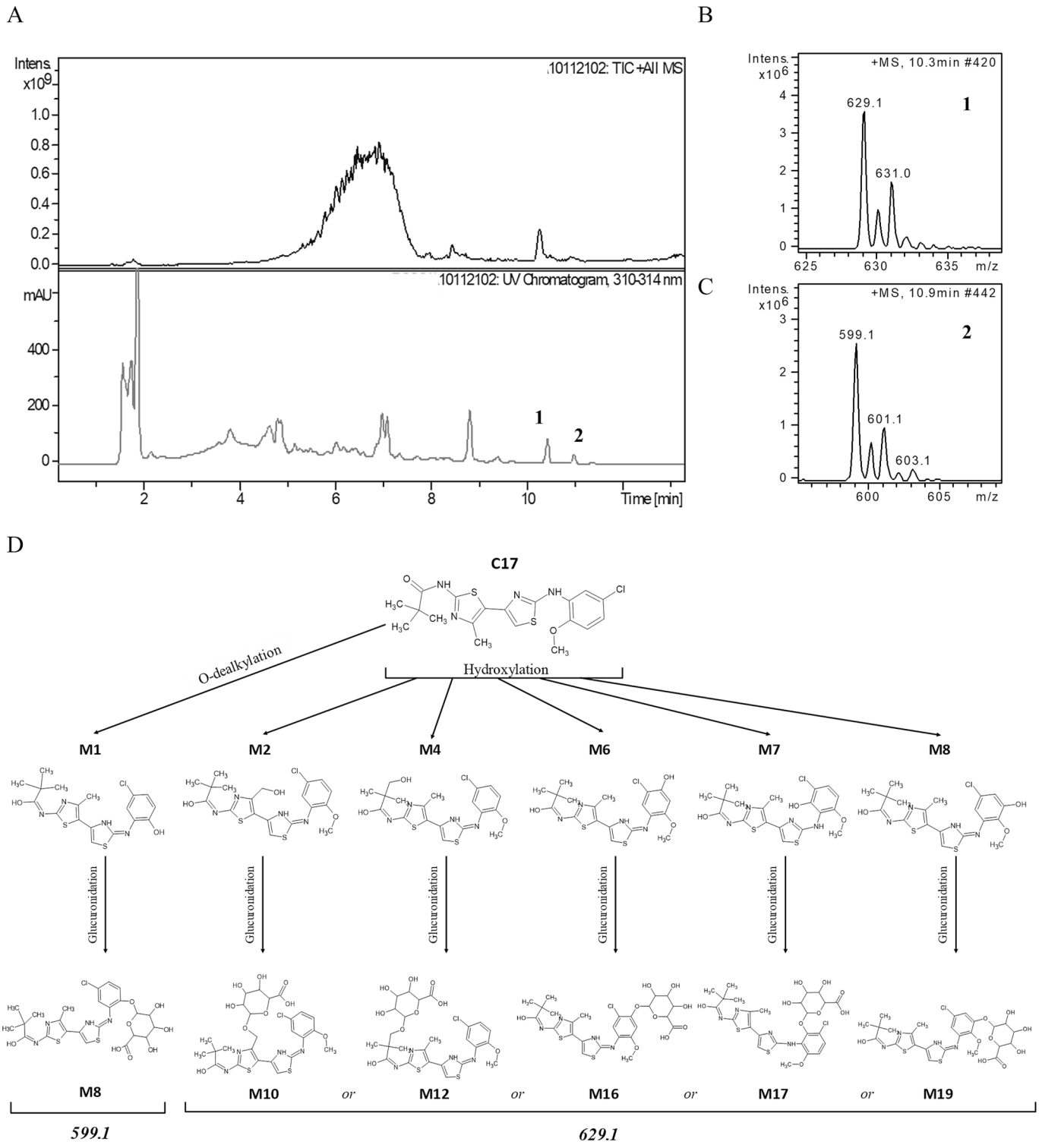

Fig. 6. HPLC-UV/ESI-MS analysis of urine from C17-treated mouse and proposed metabolic pathway of the detected metabolites. (A) Total ion current chromatogram (on the top) and UV chromatogram (on the bottom) of a representative urine sample collected 18 h after C17 administration to mice. (B, C) Mass spectra of the detected metabolites in the urine sample. (D) Proposed metabolic pathway of the detected metabolites of C17.

3.6. Chronic treatment with CFTR corrector C17

3.6.1. Recovery of the muscle force and amelioration of the dystrophic phenotype after corrector C17 treatment

The biodistribution results evidenced that after 48 h from the administration, a residual amount of C17 was still present in skeletal muscle and heart. This led us to design a chronic treatment with the LGMD2D/R3 mouse model developed by Scano et al 2022 [14] in which the administration of the compound was planned every two days, instead of the daily injection adopted in the previous tests. *Sgca*-null newborn pups were transduced in the hind limbs with AAV1 carrying the human R98H-α-SG cDNA sequence. After seven weeks, animals received an i.p. injection of 25 mg/Kg of C17 every two days for five weeks. At the end of the treatment, we assessed the muscle force of the

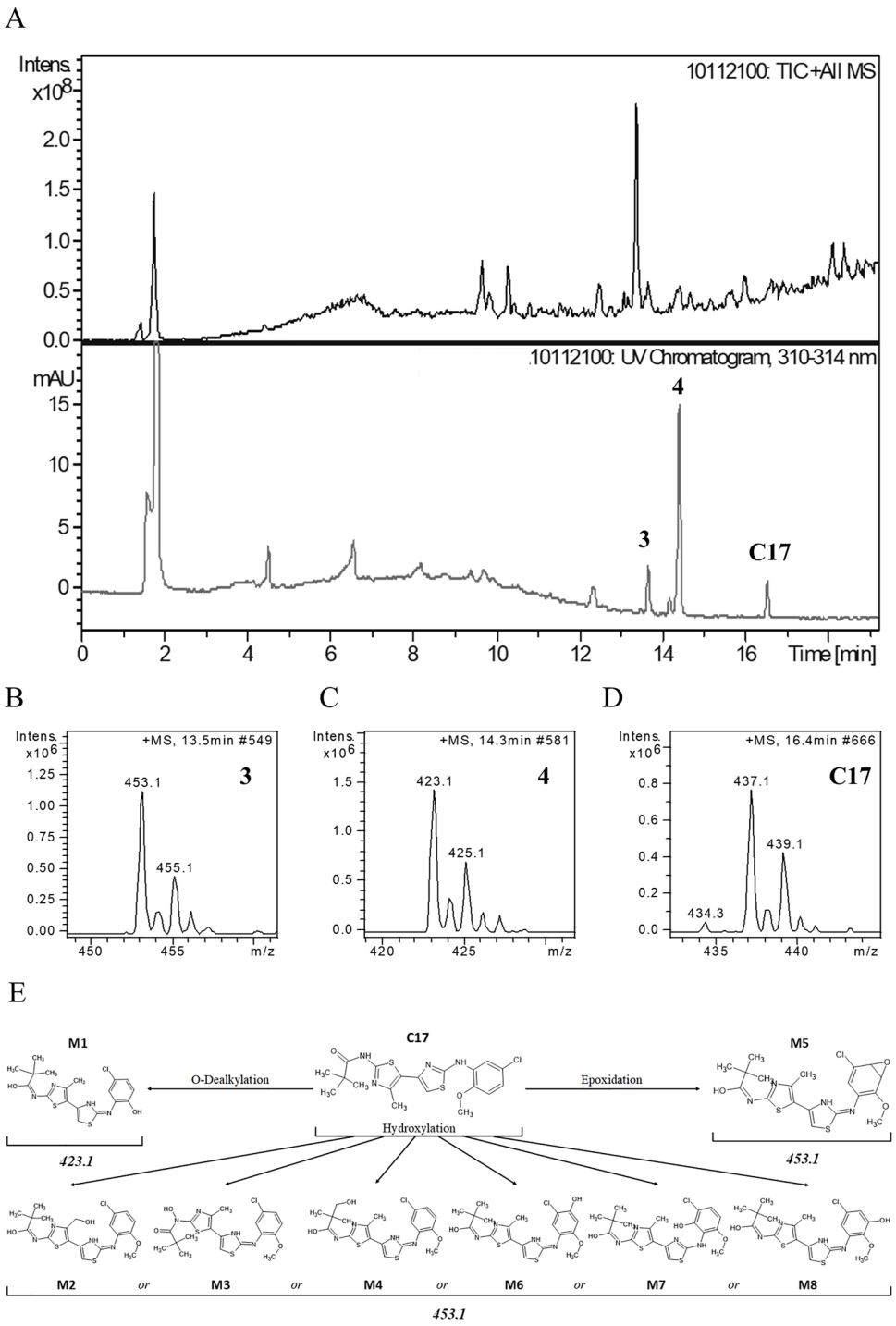

Fig. 7. HPLC-UV/ESI-MS analysis of faeces from C17-treated mouse and proposed metabolic pathways of the detected metabolites. (A) Total ion current chromatograms (on the top) and UV chromatogram (on the bottom) of a representative faeces sample collected 24 h after C17 administration. (B-D) Mass spectra of the compounds detected in the faeces. (E) Proposed metabolic pathway of the detected metabolites of C17.

Tibialis Anterior (TA) muscle. Then, mice were sacrificed, blood samples were collected, and muscles and other organs removed for histological and molecular analyses. The results confirmed the efficacy of the C17 compound for the treatment of sarcoglycanopathy also by using a lessened regimen of administration (Fig. 9A). The C17 treatment resulted in the phenotypical improvement of the muscle, with the correct localization of the human-R98H-α-SG at the sarcolemma, and consequently, the correct formation of the SG-complex, as proved by the presence of the δ-SG at the membrane (Fig. 9C). The correct localization of the SG-complex at the sarcolemma ensured the protection of the skeletal muscle during contraction, thus allowing a performance not dissimilar to the one of the wild type. Indeed from a functional point of view, the C17 treatment resulted in the increase, in comparison to the negative controls (vehicle-treated humanized and α-SG-KO mice) of the force of the TA muscle elicited *in vivo*, by the electrical stimulation of the peroneal nerve. Notably, the muscle strength of the C17 treated mice was not statistically different from that of the wild-type mice (C57BL/6J) (Fig. 9B reports the muscle strength of TA elicited at the frequency of 100 Hz).

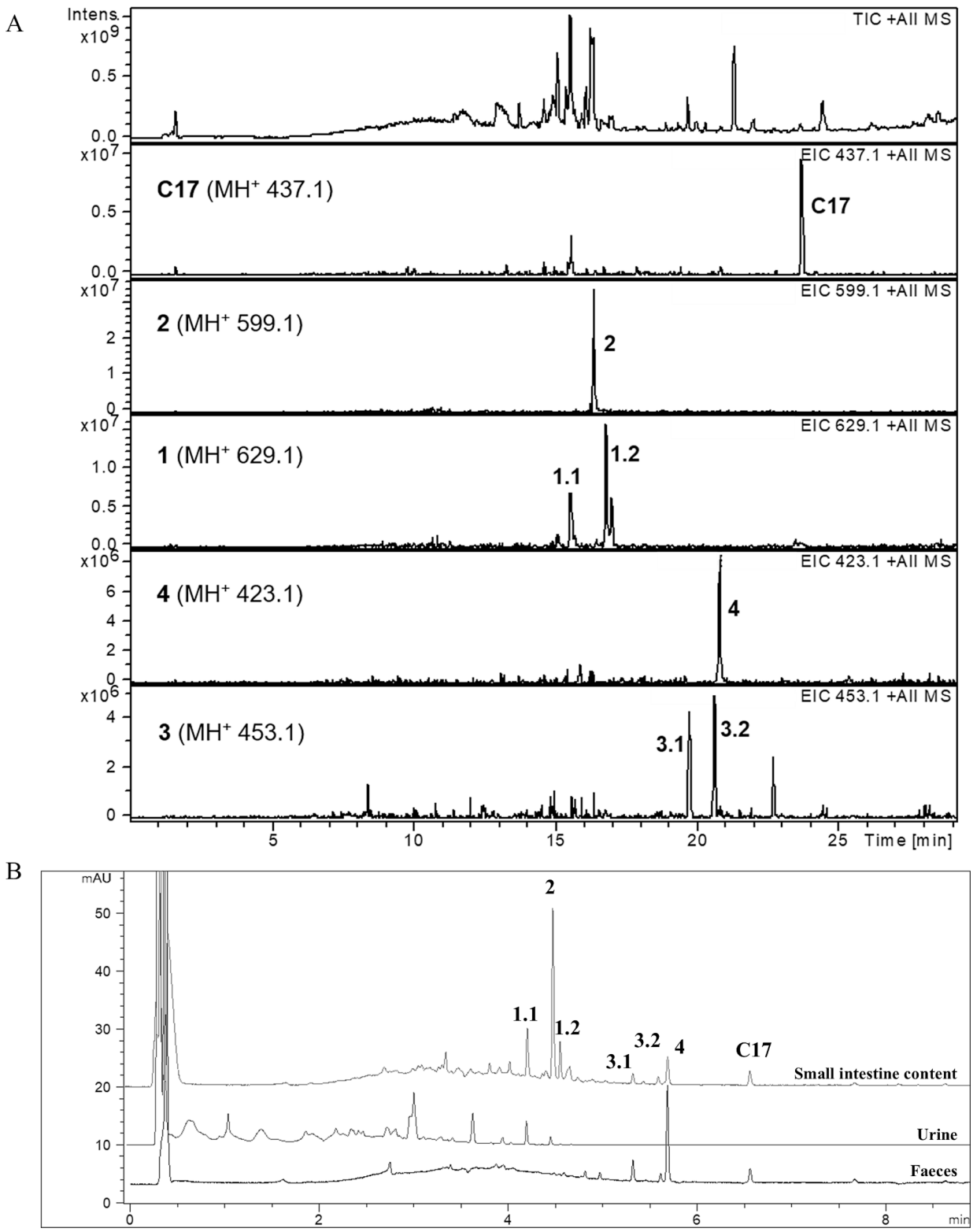

Fig. 8. HPLC-UV/ESI-MS analysis of a representative sample of gut content from C17-treated mouse and proposed metabolic pathway of the detected metabolites. (A) Total ion current chromatograms and the extracted ion chromatograms of C17 and the metabolites identified in the small intestine content collected at 24 h from treated mice. (B) Comparison of the HPLC-UV chromatograms of small intestine content, urine, and faeces from mice treated with C17.

3.6.2. Histological, hematological and biochemical analyses

Like in the chronic treatments described in [14], the administration of compound C17 did not affect the appearance, behavior, or growth of mice that were similar to the control ones, in particular the body weight increase since the start of treatment was not statistically significant between C17-treated (21.07 % ± 2.44 %) and vehicle-treated (27.43 % ± 6.49 %) humanized mice. At the end of the treatment, we also evaluated the status of the heart macroscopically and after H&E staining of cryosections, observing no sign of macroscopic and microscopic alteration in C17 treated animals in comparison to wild type, α-SG KO and

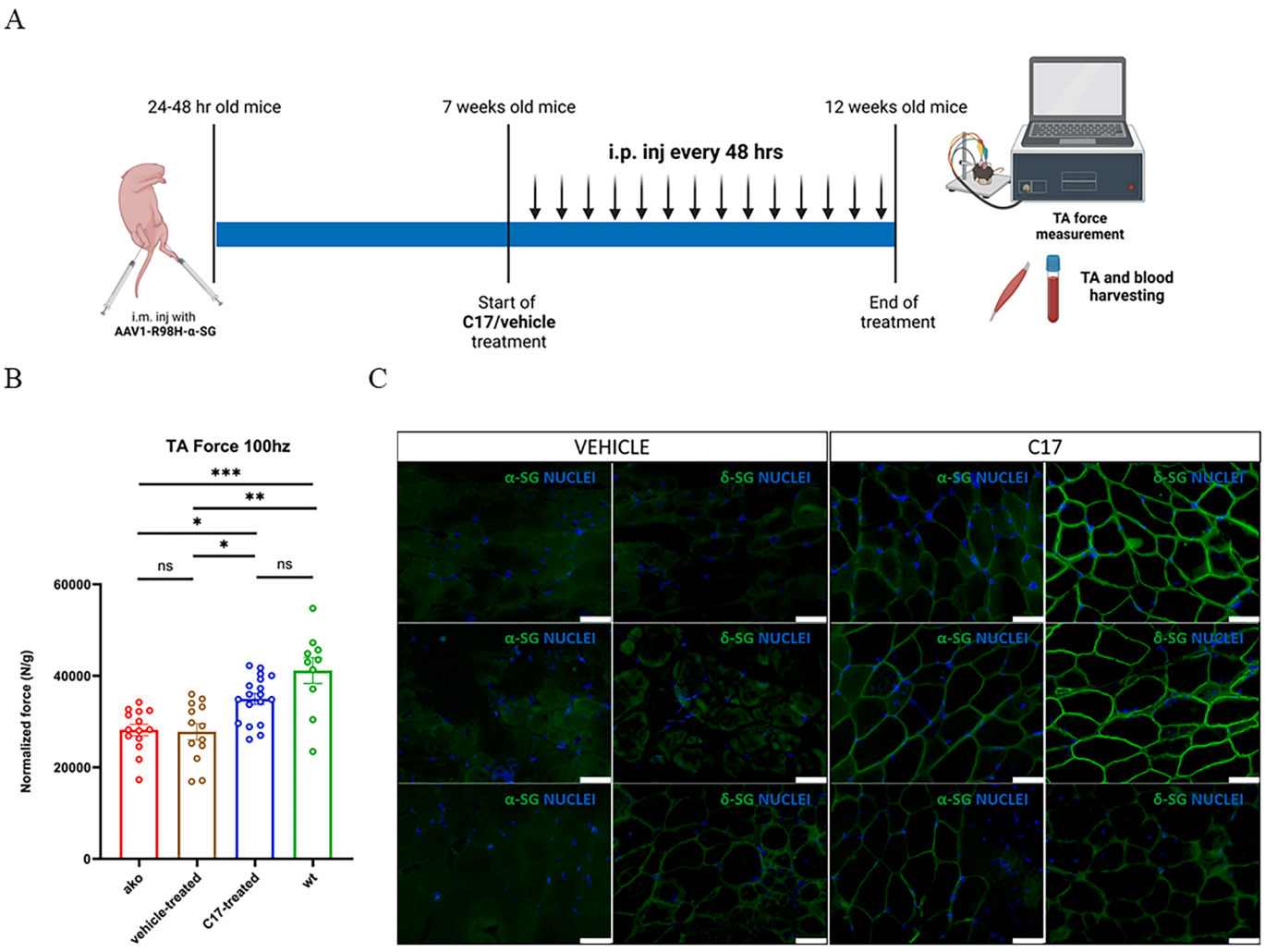

Fig. 9. Chronic treatment of 5 weeks with CFTR corrector C17. (A) Experimental work-flow (created with BioRender.com). Animals transduced as described in (Scano et al., 2022) were intraperitoneally injected (i.p.) with either C17 25 mg/kg or vehicle for 5 weeks every 48 h. At the end of the treatment, mice were tested *in vivo* for TA muscle force. Subsequently, muscles and different organs were explanted for histological and biochemical analyses. (B) Force generated by TA muscle (normalized for muscle weight) elicited by electrical stimulation of peroneal nerve at 100 Hz of WT, alpha-KO (ako), vehicle- and C17-treated mice. Each dot represents the force of a single TA muscle. Statistical analysis was performed by one-way ANOVA test followed by multiple comparisons Kruskal-Wallis's test. Data are reported as mean values ± SEM. ***, $P \leq 0.001$; **, $P \leq 0.01$; *, $P \leq 0.05$; ns, $P > 0.05$. (C) IF analysis of representative TA muscle cryo-sections of humanized mice expressing the R98H-α-SG treated for 5 weeks with either vehicle or corrector C17. All images were captured at the same setting conditions. Bar: 50 μm.

vehicle-treated ones (Fig. 10A). Furthermore, no difference was found among the different samples by measuring the apicobasal length (Fig. 10B) and the maximal width (Fig. 10C). Overall, the results indicated no obvious signs of cardiotoxicity. Hepatic and renal toxicity was already excluded in previous chronic treatments [14].

We also analyzed the blood, collected from mice at the end of the experiment, for the content of few biochemical analytes (Urea, Creatine Kinase, hemoglobin content) and the number of cells and platelets. The level of urea was similar among mice subjected to repeated compound administration and control animals, indicating that the renal filtration was not affected (Fig. 11A). RBC, WBC and platelets count were similar among all samples (Table 1), and interestingly, C17-treated mice presented a clear trend towards decreased CK level (Fig. 11B) compared to vehicle-treated mice. Creatine kinase is an indicator of the muscular damage, and this data suggests that the C17-treatment led to a beneficial effect in terms of muscular damage reduction at the level of the hindlimbs.

4. Discussion

The compound C17, whose original name is 15jf [14], has the potential to become a valuable drug, complementary to the gene transfer approach, for the treatment of the rare, and at present uncurable α-sarcoglycanopathy. The disease is characterized by the fragility of the sarcolemma, due to the loss of the structural and protective role of the SG-complex. With time, this leads to the degeneration of the skeletal muscle, the progressive worsening of normal daily activities and eventually the loss of ambulation [3]. Much effort has been devoted in recent years in the search of effective therapeutic interventions for sarcoglycanopathies. Among them, the gene replacement approach is the one that reached the most advanced stage of development, with a LGMD2D/R3 phase I/II clinical trial (NCT01976091) recently concluded and the one for LGMD2E/R4 (NCT03652259) started in 2018 still ongoing. The data of the first study [24] and the preliminary results released for the second one are promising, even though several issues are still in place, such as the amount of viral vectors needed to transduce the most abundant tissue of the body, the fact that gene replacement, for now, is one-shot therapy, and that the long term efficacy and side effects/toxicity are still unknown. On the other hand, some pharmacological approaches for sarcoglycanopathies are under preclinical study. They are based on the use of small molecules, possibly already approved for other therapeutic indications [25–27]. In this context, we have

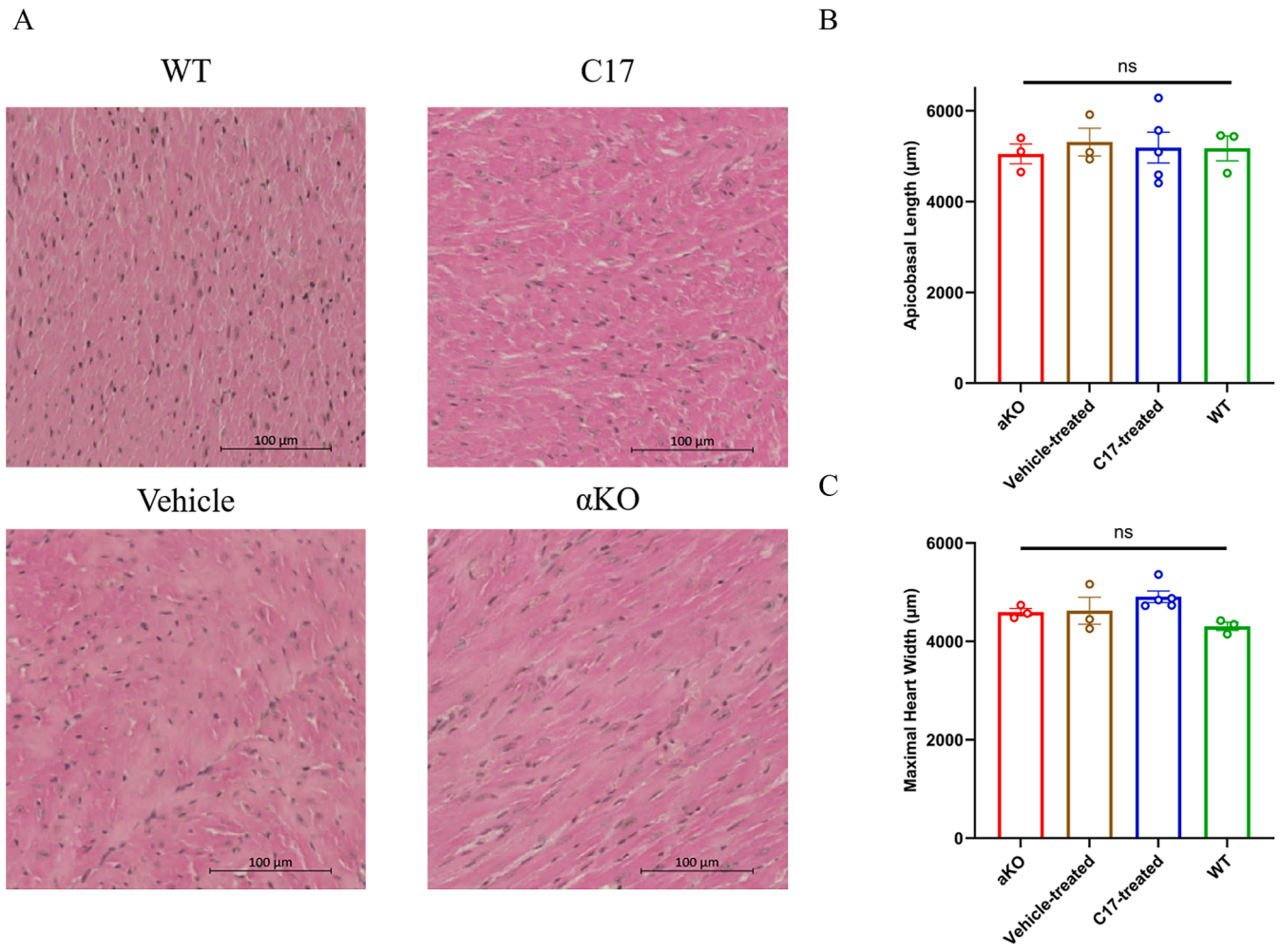

Fig. 10. Histological and morphometric analysis of heart. (A) Representative hematoxylin and eosin staining of heart sections from alpha-KO, vehicle-treated, C17-treated (C17) and wild type (WT) mice. (B and C) Morphometric measurement of the heart in terms of apicobasal length and maximal heart width (expressed in µm). Data are expressed as mean ± S.D.

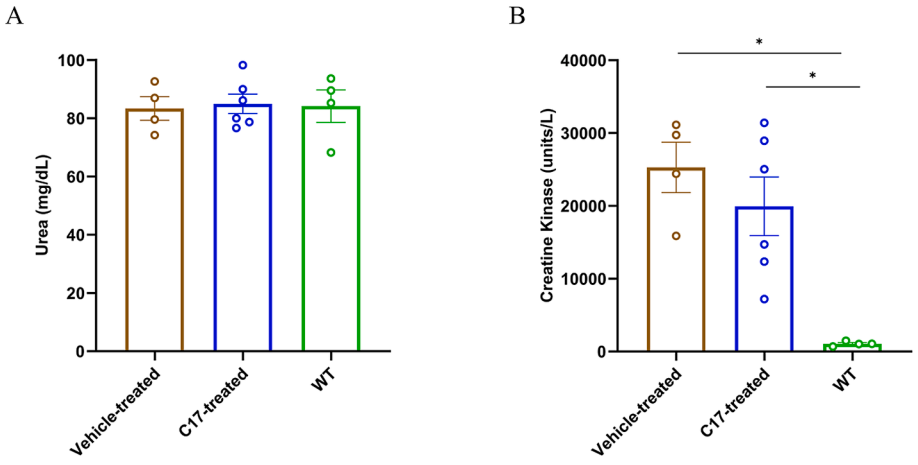

Fig. 11. Biochemical analysis. (A) Urea (mg/dL) and (B) creatine kinase (CK)(units/L) measurements in blood collected from negative control mice (vehicle-treated), C17-treated, and positive control (wild type WT) mice. Data are expressed as mean ± S.D.

evidenced that some compounds, selected to recover type II mutations of the CFTR in cystic fibrosis [28], are also effective in recovering the SG-complex at the plasma membrane [12,13]. The *in vivo* efficacy of the most promising of such small molecules, named corrector C17, has been proved in [14]. In this work, it has been generated a model in which the hind limbs expressed a human mutated form of α-SG thanks to AAV-transduction. The work shows that the recovery of skeletal muscle strength in the hind limbs of the humanized mouse model of LGMD2D/R3 was the result of the re-localization at the sarcolemma of a functional SG-complex, despite containing a mutated α-SG [14]. Because of these

Table 1

Haematological analysis. Haematocrit of C17-treated, vehicle-treated, alpha-KO and wild-type mice. MPV, mean platelet volume; PDW, platelet distribution width; PLT, platelet count; WBC, white blood cells; RBC, red blood cells; HGB, haemoglobin; HCT, haematocrit test; MCV, mean corpuscular volume; MCH, mean corpuscular haemoglobin; MCHC, mean corpuscular haemoglobin concentration; CHCM: mean cellular haemoglobin concentration; RDW, red cell distribution; HDW, haemoglobin distribution width. Statistical analysis was performed by One-Way ANOVA test followed by multiple comparisons of Kruskal-Wallis's test. Data are reported as mean values ± S.D.; *, $P \leq 0.05$; ns, $P > 0.05$.

	C17-treated (n = 6)	Vehicle-treated (n = 5)	aKO (n = 4)	WT (n = 4)	Ordinary One-way Anova
Neutrophils [%]	19.45 ± 7.62	24 ± 7.18	17.5 ± 5	14.25 ± 8.42	ns
Lymphocytes [%]	71.18 ± 11.95	68.8 ± 6.06	77.5 ± 7.55	76.5 ± 8.70	ns
Monocytes [%]	7.70 ± 5.387	6.2 ± 3.834	4.00 ± 3.27	6.75 ± 2.75	ns
Eosinophils [%]	1.67 ± 1.97	1.00 ± 1	1.00 ± 2.00	2.50 ± 1.00	ns
Neutrophils [10^3 cell/μL]	0.44 ± 0.147	0.78 ± 0.51	0.41 ± 0.182	0.64 ± 0.63	ns
Lymphocytes [10^3 cell/μL]	1.73 ± 0.681	2.09 ± 0.91	1.82 ± 0.78	2.72 ± 1.54	ns
Monocytes [10^3 cell/μL]	0.19 ± 0.13	0.17 ± 0.12	0.12 ± 0.15	0.24 ± 0.12	ns
Eosinophils [10^3 cell/μL]	0.045 ± 0.054	0.028 ± 0.026	0.040 ± 0.080	0.087 ± 0.040	ns
MPV [fL]	8.9 ± 0.71	9.14 ± 0.85	8.95 ± 0.51	8.43 ± 0.48	ns
PDW [%]	47.22 ± 2.76	50.22 ± 5.86	48.00 ± 2.90	50.73 ± 3.56	ns
PLT [%]	1.26 ± 0.18	1.25 ± 0.31	1.30 ± 0.10	0.83 ± 0.16	* ($p < 0.05$), WT vs aKO/ vehicle/C17
WBC [10^3 cell/μL]	2.39 ± 0.72	3.06 ± 1.38	2.38 ± 1.14	3.69 ± 2.28	Ns
RBC [10^6 cell/μL]	9.79 ± 0.65	9.76 ± 0.73	10.85 ± 0.49	10.20 ± 0.71	Ns
HGB [g/dL]	13.40 ± 0.90	13.44 ± 0.54	14.80 ± 0.86	14.60 ± 0.95	Ns
HCT [%]	42.73 ± 2.55	42.00 ± 2.37	47.40 ± 1.77	45.40 ± 2.72	* ($p < 0.05$), vehicle vs aKO
MCV [fL]	43.70 ± 0.99	43.06 ± 1.72	43.73 ± 0.48	44.63 ± 0.46	Ns
MCH [pg]	13.73 ± 0.48	13.90 ± 1.04	13.70 ± 0.22	14.30 ± 0.25	Ns
MCHC [g/dL]	31.37 ± 0.92	32.30 ± 2.70	31.30 ± 0.80	32.03 ± 0.47	Ns
CHCM [g/dL]	33.17 ± 2.33	32.74 ± 2.61	32.35 ± 1.73	33.15 ± 1.63	Ns
CH [pg]	14.45 ± 0.74	13.98 ± 0.64	14.10 ± 0.61	14.75 ± 0.85	Ns
RDW [%]	13.92 ± 0.52	14.58 ± 0.95	13.30 ± 0.60	13.03 ± 0.79	* ($p < 0.05$), WT vs vehicle
HDW [g/dL]	1.99 ± 0.23	2.04 ± 0.21	1.91 ± 0.10	1.95 ± 0.14	Ns
PLT [10^3 cell/μL]	1411.3 ± 147.3	1368.8 ± 266.9	1459.0 ± 150.5	984.0 ± 169.4	* ($p < 0.05$), WT vs aKO/ vehicle/C17

promising results, C17 deserves further attention. However, corrector C17 is not among the ones presently approved for treating cystic fibrosis [29]. We, therefore, analyzed the pharmacokinetic properties of the compound, highlighting that C17, after an acute administration in mice, first reached the most vascularized organs (liver, kidneys, spleen) and then, through the circulation, was redistributed to the entire body. The concentration–time kinetic relationship of C17 in plasma and other tissues was in accordance with the route of administration and the small molecule was still detectable in the target tissues (skeletal muscle and heart) 48 h post injection. This allowed us to successfully perform a new efficacy test in which chronic administration in the humanized LGMD2D/R3 model was performed via i.p. injection every two days instead of every day. We can also say that the compound is safe, according to the results on mice. These experiments showed that the sarcolemma in the hind limbs of treated mice is less fragile compared to that of untreated mice. This finding is significant because, along with improving muscle function, there was also a decrease in the blood levels of CK, an enzyme that indicates muscle damage. Although the difference in enzyme levels is not statistically significant, it is important to note that the C17 treatment specifically benefits the humanized hind limb muscles, which produce the α-SG protein, even if it is mutated. Conversely, the remaining skeletal muscle tissue in the *sgca*-null mice, which served as the background for transduction, is completely deficient in the α-SG subunit, and is likely the source of the creatine kinase being released. We found no C17 metabolites in the tissues analyzed, except the gut, and no C17 derivative was observed by performing *in vitro* tests with extracts from livers of both murine and human origin. On the other hand, regarding the elimination process from the body, C17 presents some similarities with other CFTR modulators, indeed, like Ivacaftor, Tezacaftor and Elexacaftor, components of Trikafta®, the small molecule is excreted in the faeces both unmodified and after conversion, whereas a small amount of modified C17 can be found in the urine [30]. The molecule is highly hydrophobic and thus is not surprising to find the unmodified C17 in the faeces. On the other hand, the compounds found in the urine are extensively modified to render the C17 structure more hydrophilic so that after being re-absorbed in the small intestine, can be secreted in the urine. All things considered, C17 has great potential to become an effective drug in the treatment of sarcoglycanopathies, complementary to the gene therapy approach. Of course, this pharmacological strategy would be applied to the forms of the disease caused by a genetic defect leading to the production of a folding defective but potentially functional α-SG. According to what has been reported in the LOVD[3] (Leiden Open Variation Database) system and recently reviewed in [5], this kind of mutations accounts for about 69 % of all the *SGCA* defects. Furthermore, it is known that in sarcoglycanopathy there is a high degree of compound heterozygosity, with different mutations on the two alleles of the gene involved. This increases the number of LGMD2D/R3 subjects who can benefit from the application of the corrector C17 because it would be sufficient the recovery of just one of the two mutated allele products to improve the phenotype. Furthermore, the possibility of using myogenic cells from sarcoglycanopathy subjects, like in [12,13], will be of great help in evaluating the efficacy of C17 on a specific *SGCA* mutation, thus tailoring the treatment to the predicted response of the individual patient.

Corrector C17 belongs to the family of bithiazole derivatives that are supposed to promote the rescue of CFTR mutants through at least two mechanisms, by directly interacting with the chloride channel at the bithiazole binding site of the nucleotide binding domain 2 (NBD2), and/or by promoting the folding and glycosylation of the transmembrane domains (TMDs) [31,32]. While in the first case, C17 can be classified as a classical pharmacological chaperone, in the second one it could act either directly or indirectly as a proteostasis regulator. This last mechanism of action is also supported by subsequent evidence that C17 can rescue proteins structurally similar or structurally uncorrelated to the CFTR [33–35]. α-SG is a small type I transmembrane protein with no structural similarity to CFTR [6,36,37]. Thus, we can argue that the rescue of α-SG by C17 is mainly due to a general mechanism, which could modulate the activity, composition or concentration of elements of the proteostasis network. If this is true, and the process of development of C17 as a drug will end with the approval for the treatments of LGMD2D/R3 by the regulatory agencies, the repurposing of this small molecule for other indications will be straightforward, shortening the gap towards a cure for several rare genetic diseases.

CRediT authorship contribution statement

Alberto Benetollo: Writing – original draft, Methodology, Investigation, Formal analysis, Data curation, Conceptualization. **Sofia Parrasia:** Validation, Methodology, Formal analysis. **Martina Scano:** Visualization, Methodology, Data curation. **Lucia Biasutto:** Validation, Software, Methodology. **Andrea Rossa:** Methodology. **Leonardo Nogara:** Methodology, Data curation. **Bert Blaauw:** Validation, Formal analysis. **Francesco Dalla Barba:** Methodology, Data curation. **Paola Caccin:** Visualization, Methodology. **Marcello Carotti:** Validation, Methodology. **Alessandro Parolin:** Methodology. **Eylem Emek Akyurek:** Visualization, Methodology. **Roberta Sacchetto:** Validation. **Dorianna Sandonà:** Writing – review & editing, Validation, Supervision, Project administration, Funding acquisition, Formal analysis, Conceptualization.

Declaration of competing interest

The authors declare that they have no known competing financial interests or personal relationships that could have appeared to influence the work reported in this paper.

Acknowledgements

This work was supported by the Association Françoise contre les Myopathies, France, AFM Grant #23000, AFM Grant #28892; the Muscular Dystrophy Association, United States, Grant #MDA 577888, (https://doi.org/10.55762/pc.gr.81540); the Italian Telethon Foundation, Italy, GGP20097. Figures in this work were created with biorender.com. The authors would like to thank Mr. Mauro Ghidotti for the valuable help and advices in animal handling.

References

[1] V. Straub, A. Murphy, B. Udd, L.w.s. group, 229th ENMC international workshop: Limb girdle muscular dystrophies - Nomenclature and reformed classification Naarden, the Netherlands, 17-19 March 2017, Neuromuscul. Disord. 28 (2018) 702–710, https://doi.org/10.1016/j.nmd.2018.05.007.

[2] D. Sandona, R. Betto, Sarcoglycanopathies: molecular pathogenesis and therapeutic prospects, Expert Rev Mol Med 11 (2009) e28.

[3] M. Vainzof, L.S. Souza, J. Gurgel-Giannetti, M. Zatz, Sarcoglycanopathies: an update, Neuromuscul. Disord. 31 (2021) 1021–1027, https://doi.org/10.1016/j.nmd.2021.07.014.

[4] P. Narayanaswami, M. Weiss, D. Selcen, W. David, E. Raynor, G. Carter, M. Wicklund, R.J. Barohn, E. Ensrud, R.C. Griggs, G. Gronseth, A.A. Amato, N. Guideline Development Subcommittee of the American Academy of, N. Practice Issues Review Panel of the American Association of, M. Electrodiagnostic, Evidence-based guideline summary: diagnosis and treatment of limb-girdle and distal dystrophies: report of the guideline development subcommittee of the American Academy of Neurology and the practice issues review panel of the American Association of Neuromuscular & Electrodiagnostic Medicine, Neurology 83 (2014) 1453–1463, https://doi.org/10.1212/WNL.0000000000000892.

[5] M. Scano, A. Benetollo, F. Dalla Barba, D. Sandona, Advanced therapeutic approaches in sarcoglycanopathies, Curr. Opin. Pharmacol. 76 (2024) 102459, https://doi.org/10.1016/j.coph.2024.102459.

[6] M. Carotti, C. Fecchio, D. Sandona, Emerging therapeutic strategies for sarcoglycanopathy, Expert Opin. Orphan D 5 (2017) 381–396, https://doi.org/10.1080/21678707.2017.1307731.

[7] M. Bartoli, E. Gicquel, L. Barrault, T. Soheili, M. Malissen, B. Malissen, N. Vincent-Lacaze, N. Perez, B. Udd, O. Danos, I. Richard, Mannosidase I inhibition rescues the human alpha-sarcoglycan R77C recurrent mutation, Hum. Mol. Genet. 17 (2008) 1214–1221, https://doi.org/10.1093/hmg/ddn029.

[8] S. Gastaldello, S. D'Angelo, S. Franzoso, M. Fanin, C. Angelini, R. Betto, D. Sandona, Inhibition of proteasome activity promotes the correct localization of disease-causing alpha-sarcoglycan mutants in HEK-293 cells constitutively expressing beta-, gamma-, and delta-sarcoglycan, Am. J. Pathol. 173 (2008) 170–181, https://doi.org/10.2353/ajpath.2008.071146.

[9] T. Soheili, E. Gicquel, J. Poupiot, L. N'Guyen, F. Le Roy, M. Bartoli, I. Richard, Rescue of sarcoglycan mutations by inhibition of endoplasmic reticulum quality control is associated with minimal structural modifications, Hum. Mutat. 33 (2012) 429–439, https://doi.org/10.1002/humu.21659.

[10] E. Bianchini, M. Fanin, K. Mamchaoui, R. Betto, D. Sandonà, Unveiling the degradative route of the V247M α-sarcoglycan mutant responsible for LGMD-2D, Hum. Mol. Genet. 23 (2014) 3746–3758, https://doi.org/10.1093/hmg/ddu088.

[11] M. Lopes-Pacheco, N. Pedemonte, G. Veit, Discovery of CFTR modulators for the treatment of cystic fibrosis, Expert Opin. Drug Discov. 16 (2021) 897–913, https://doi.org/10.1080/17460441.2021.1912732.

[12] M. Carotti, M. Scano, I. Fancello, I. Richard, G. Risato, M. Bensalah, M. Soardi, D. Sandona, Combined use of CFTR correctors in LGMD2D myotubes improves sarcoglycan complex recovery, Int. J. Mol. Sci. 21 (2020), https://doi.org/10.3390/ijms21051813.

[13] M. Carotti, J. Marsolier, M. Soardi, E. Bianchini, C. Gomiero, C. Fecchio, S. F. Henriques, R. Betto, R. Sacchetto, I. Richard, D. Sandona, Repairing folding-defective alpha-sarcoglycan mutants by CFTR correctors, a potential therapy for limb-girdle muscular dystrophy 2D, Hum. Mol. Genet. 27 (2018) 969–984, https://doi.org/10.1093/hmg/ddy013.

[14] M. Scano, A. Benetollo, L. Nogara, M. Bondi, F. Dalla Barba, M. Soardi, S. Furlan, E. E. Akyurek, P. Caccin, M. Carotti, R. Sacchetto, B. Blaauw, D. Sandona, CFTR corrector C17 is effective in muscular dystrophy, in vivo proof of concept in LGMDR3, Hum. Mol. Genet. 31 (2022) 499–509, https://doi.org/10.1093/hmg/ddab260.

[15] Y. Djoumbou-Feunang, J. Fiamoncini, A. Gil-de-la-Fuente, R. Greiner, C. Manach, D.S. Wishart, BioTransformer: a comprehensive computational tool for small molecule metabolism prediction and metabolite identification, J. Cheminf. 11 (2019) 2, https://doi.org/10.1186/s13321-018-0324-5.

[16] D.S. Wishart, S. Tian, D. Allen, E. Oler, H. Peters, V.W. Lui, V. Gautam, Y. Djoumbou-Feunang, R. Greiner, T.O. Metz, BioTransformer 3.0-a web server for accurately predicting metabolic transformation products, Nucleic Acids Res. 50 (2022) W115–W123, https://doi.org/10.1093/nar/gkac313.

[17] L. Jia, X. Liu, The conduct of drug metabolism studies considered good practice (II): In vitro experiments, Curr. Drug Metab. 8 (2007) 822–829, https://doi.org/10.2174/138920007782798207.

[18] A. Al Shoyaib, S.R. Archie, V.T. Karamyan, Intraperitoneal route of drug administration: Should it be used in experimental animal studies? Pharm. Res. 37 (2020) 12, https://doi.org/10.1007/s11095-019-2745-x.

[19] D. Chen, J. Yu, Z. Zhang, X. Su, L. Li, L. Li, Controlling preanalytical process in high-coverage quantitative metabolomics: spot-sample collection for mouse urine and fecal metabolome profiling, Anal. Chem. 91 (2019) 4958–4963, https://doi.org/10.1021/acs.analchem.9b00310.

[20] G.A. Reed, Stability of drugs, drug candidates, and metabolites in blood and plasma, Curr Protoc Pharmacol 75 (2016), https://doi.org/10.1002/cpph.16.

[21] E.K. Schneider, F. Reyes-Ortega, J. Li, T. Velkov, Can cystic fibrosis patients finally catch a breath with lumacaftor/ivacaftor? Clin. Pharmacol. Ther. 101 (2017) 130–141, https://doi.org/10.1002/cpt.548.

[22] E.F.A. Brandon, C.D. Raap, I. Meijerman, J.H. Beijnen, J.H.M. Schellens, An update on in vitro test methods in human hepatic drug biotransformation research: pros and cons, Toxicol. Appl. Pharmacol. 189 (2003) 233–246, https://doi.org/10.1016/S0041-008X(03)00128-5.

[23] I. Ogobuiro, J. Gonzales, K.R. Shumway, F. Tuma, Physiology, Gastrointestinal, StatPearls, Treasure Island (FL), 2024.

[24] J.R. Mendell, L.G. Chicoine, S.A. Al-Zaidy, Z. Sahenk, K. Lehman, L. Lowes, N. Miller, L. Alfano, B. Galliers, S. Lewis, D. Murrey, E. Peterson, D.A. Griffin, K. Church, S. Cheatham, J. Cheatham, M.J. Hogan, L.R. Rodino-Klapac, Gene delivery for limb-girdle muscular dystrophy type 2D by isolated limb infusion, Hum. Gene Ther. 30 (2019) 794–801, https://doi.org/10.1089/hum.2019.006.

[25] G. Careccia, M. Saclier, M. Tirone, E. Ruggieri, E. Principi, L. Raffaghello, S. Torchio, D. Recchia, M. Canepari, A. Gorzanelli, M. Ferrara, P. Castellani, A. Rubartelli, P. Rovere-Querini, M. Casalgrandi, A. Preti, I. Lorenzetti, C. Bruno, R. Bottinelli, S. Brunelli, S.C. Previtali, M.E. Bianchi, G. Messina, E. Venereau, Rebalancing expression of HMGB1 redox isoforms to counteract muscular dystrophy, Sci. Transl. Med. 13 (2021), https://doi.org/10.1126/scitranslmed.aay8416.

[26] L. Raffaghello, E. Principi, S. Baratto, C. Panicucci, S. Pintus, F. Antonini, G. Del Zotto, A. Benzi, S. Bruzzone, P. Scudieri, C. Minetti, E. Gazzerro, C. Bruno, P2X7 Receptor Antagonist Reduces Fibrosis and Inflammation in a Mouse Model of Alpha-Sarcoglycan Muscular Dystrophy, Pharmaceuticals (Basel) 15 (2022), https://doi.org/10.3390/ph15010089.

[27] J. Alonso-Perez, A. Carrasco-Rozas, M. Borrell-Pages, E. Fernandez-Simon, P. Pinol-Jurado, L. Badimon, L. Wollin, C. Lleixa, E. Gallardo, M. Olive, J. Diaz-Manera, X. Suarez-Calvet, Nintedanib reduces muscle fibrosis and improves muscle function of the alpha-sarcoglycan-deficient mice, Biomedicines 10 (2022), https://doi.org/10.3390/biomedicines10102629.

[28] K. Fiedorczuk, J. Chen, Mechanism of CFTR correction by type I folding correctors, Cell 185 (2022) 158–168 e111, https://doi.org/10.1016/j.cell.2021.12.009.

[29] H.G.M. Heijerman, E.F. McKone, D.G. Downey, E. Van Braeckel, S.M. Rowe, E. Tullis, M.A. Mall, J.J. Welter, B.W. Ramsey, C.M. McKee, G. Marigowda, S. M. Moskowitz, D. Waltz, P.R. Sosnay, C. Simard, N. Ahluwalia, F. Xuan, Y. Zhang, J.L. Taylor-Cousar, K.S. McCoy, V.X.T. Group, Efficacy and safety of the elexacaftor plus tezacaftor plus ivacaftor combination regimen in people with cystic fibrosis homozygous for the F508del mutation: a double-blind, randomised, phase 3 trial, Lancet 394 (2019) 1940–1948, https://doi.org/10.1016/S0140-6736(19)32597-8.

[30] R.v.d. Meer, CFTR Modulators: Does one dose fit all? J. Pers. Med. (2021) https://doi.org/10.3390/jpm11060458.

[31] T.W. Loo, M.C. Bartlett, L. Shi, D.M. Clarke, Corrector-mediated rescue of misprocessed CFTR mutants can be reduced by the P-glycoprotein drug pump, Biochem. Pharmacol. 83 (2012) 345–354, https://doi.org/10.1016/j.bcp.2011.11.014.

[32] T.W. Loo, M.C. Bartlett, D.M. Clarke, Bithiazole correctors rescue CFTR mutants by two different mechanisms, Biochemistry 52 (2013) 5161–5163, https://doi.org/10.1021/bi4008758.

[33] W.L. van der Woerd, C.G.K. Wichers, A.L. Vestergaard, J.P. Andersen, C. C. Paulusma, R.H.J. Houwen, S.F.J. van de Graaf, Rescue of defective ATP8B1 trafficking by CFTR correctors as a therapeutic strategy for familial intrahepatic cholestasis, J. Hepatol. 64 (2016) 1339–1347, https://doi.org/10.1016/j.jhep.2016.02.001.

[34] S. Kinting, S. Hoppner, U. Schindlbeck, M.E. Forstner, J. Harfst, T. Wittmann, M. Griese, Functional rescue of misfolding ABCA3 mutations by small molecular correctors, Hum. Mol. Genet. 27 (2018) 943–953, https://doi.org/10.1093/hmg/ddy011.

[35] A. Ben Saad, V. Vauthier, A. Toth, A. Janaszkiewicz, A.M. Durand-Schneider, A. Bruneau, J.L. Delaunay, M. Lapalus, E. Mareux, I. Garcin, E. Gonzales, C. Housset, T. Ait-Slimane, E. Jacquemin, F. Di Meo, T. Falguieres, Effect of CFTR correctors on the traffic and the function of intracellularly retained ABCB4 variants, Liver Int. 41 (2021) 1344–1357, https://doi.org/10.1111/liv.14839.

[36] N.J. Dickens, S. Beatson, C.P. Ponting, Cadherin-like domains in alpha-dystroglycan, alpha/epsilon-sarcoglycan and yeast and bacterial proteins, Curr. Biol. 12 (2002) R197–R199.

[37] N. Cant, N. Pollock, R.C. Ford, CFTR structure and cystic fibrosis, Int. J. Biochem. Cell Biol. 52 (2014) 15–25, https://doi.org/10.1016/j.biocel.2014.02.004.

[38] ChemSketch, version 2022.1.2, Advanced Chemistry Development, Inc. (ACD/Labs), Toronto, ON, Canada, www.acdlabs.com.